HHS Public Access

Author manuscript

Biochim Biophys Acta Mol Cell Biol Lipids. Author manuscript; available in PMC 2023 July 01.

Published in final edited form as:

Biochim Biophys Acta Mol Cell Biol Lipids. 2023 January ; 1868(1): 159238. doi:10.1016/j.bbalip.2022.159238.

The proximal intestinal Fatty Acid-Binding Proteins liver FABP (LFABP) and intestinal FABP (IFABP) differentially modulate whole body energy homeostasis but are not centrally involved in net dietary lipid absorption: Studies of the LFABP/IFABP double knockout mouse☆

Angela M. Gajda[a,b,1], **Hiba R. Tawfeeq**[a,b,1,2], **Atreju I. Lackey**[a,b], **Yin Xiu Zhou**[a], **Hamzeh Kanaan**[a], **Arete Pappas**[a], **Heli Xu**[a,b], **Sarala Kodukula**[a], **Judith Storch**[a,b,*]

[a]Department of Nutritional Sciences, Rutgers University, New Brunswick, NJ 08901, USA

[b]Rutgers Center for Lipid Research, Rutgers University, New Brunswick, NJ 08901, USA

Abstract

Proximal intestinal enterocytes expresses both intestinal-fatty acid binding protein (IFABP; FABP2) and liver-FABP (LFABP; FABP1). These FABPs are thought to be important in the net uptake of dietary lipid from the intestinal lumen, however their specific and potentially unique functions in the enterocyte remain incompletely understood. We previously showed markedly divergent phenotypes in LFABP$^{-/-}$ vs. IFABP$^{-/-}$ mice fed high-fat diets, with the former becoming obese and the latter remaining lean relative to wild-type (WT) mice, supporting different functional roles for each protein. Interestingly, neither mouse model displayed increased fecal lipid concentration, raising the question of whether the presence of one FABP was sufficient to compensate for absence of the other. Here, we generated an LFABP and IFABP double knockout mouse (DKO) to determine whether simultaneous ablation would lead to fat malabsorption, and to further interrogate the individual vs. overlapping functions of these proteins. Male WT, IFABP$^{-/-}$, LFABP$^{-/-}$, and DKO mice were fed a low-fat (10 % kcal) or high-fat (45 % kcal) diet for 12 weeks. The body weights and fat mass of the DKO mice integrated those of the LFABP$^{-/-}$ and IFABP$^{-/-}$ single knockouts, supporting the notion that IFABP and LFABP have distinct functions in intestinal lipid assimilation that result in downstream alterations in systemic energy metabolism. Remarkably, no differences in fecal fat concentrations were found in the DKO compared to WT, revealing that the FABPs are not required for net intestinal uptake of dietary lipid.

☆This article is part of a Special Issue entitled Intestinal Lipid Metabolism in Health and Disease edited by Dr. Kimberly Buhman.

*Corresponding author at: Department of Nutritional Sciences, Rutgers University, 65 Dudley Road, New Brunswick, NJ 08901, USA. Storch@sebs.rutgers.edu (J. Storch).

[1]These authors contributed equally to this work.

[2]Present address: College of Pharmacy, University of Mosul, Mosul 41002, Iraq.

CRediT authorship contribution statement

A.M.G. and H.R.T.: conceptualization, investigation, methodology, visualization, data curation and interpretation, writing - original draft preparation, reviewing and editing; A.I.L. and H.X.: investigation, methodology, data curation and interpretation; Y.X.Z. and S.K.: investigation, methodology; H.K. and A.P.: investigation; J.S.: conceptualization, visualization, data curation and interpretation, writing - original and final draft preparation, reviewing and editing, resources, supervision, funding acquisition, project administration.

Declaration of competing interest

No conflicts of interest, financial or otherwise, are declared by the authors.

Keywords

Lipid; Monoacyglycerol; Fatty acid; Fatty acid binding protein; Intestinal metabolism; Lipid absorption

1. Introduction

The enterocyte of the proximal small intestine is the major site of absorption of diet-derived lipids, with an efficiency of >95 %. Hydrolysis of dietary triglyceride (TG) by lipases in the intestinal lumen results in the release of fatty acids (FA) and monoacyglycerols (MG) [1]. These hydrophobic molecules enter the absorptive enterocytes of the small intestine, and soluble carrier proteins are believed to be necessary for their transport through the hydrophilic environment of the cytosol to access various metabolic processes including oxidation, reesterification, and storage [2]. In the intestinal enterocyte, two FABPs are present: Liver FABP (LFABP; FABP1) and Intestinal FABP (IFABP; FABP2). LFABP was initially discovered in the liver, but was soon found to be highly expressed in the intestine also. IFABP is solely expressed in the small intestine, with intestinal expression levels similar to LFABP in the mouse [3,4].

Although identified about 50 years ago, the individual functions of IFABP and LFABP are not definitively understood, thus it remains unclear why the same cell type expresses two structurally similar, evolutionarily related proteins. IFABP is typical of the FABP family in that it has a single high affinity binding site for FA, whereas LFABP is unique in that it can bind two FAs simultaneously; LFABP also binds two MGs, and several other hydrophobic ligands [5,6]. LFABP binds unsaturated FA with somewhat greater affinity than IFABP [7,8]. Additionally, both IFABP and LFABP have been found to bind endocannabinoids (ECs) [9,10]. Kinetics studies have shown that LFABP transfers FA to model membranes via an aqueous diffusional mechanism, while IFABP interacts directly with membranes during FA transfer [11–13]. Such differences in ligand binding affinities and transfer mechanisms have led to the hypothesis that these intracellular proteins may have different functions in the enterocyte.

Intestinal expression of LFABP does not increase in the absence of IFABP, and vice-versa [14,15]; the absence of compensation provides further evidence, albeit indirect, that these proteins have different functions. The hypothesis was critically examined by directly comparing mice null for LFABP and mice null for IFABP. High-fat diet (HFD) feeding of $LFABP^{-/-}$ vs $IFABP^{-/-}$ mice revealed robust phenotypic differences. $LFABP^{-/-}$ mice became obese and hyperphagic; this was potentially due, at least in part, to higher mucosal ECs levels which would promote higher food intake. By contrast, $IFABP^{-/-}$ mice remained lean, regardless of dietary fat amount or type [16]. The lower respiratory exchange ratios (RER) in $LFABP^{-/-}$ mice relative to wild-type (WT) mice suggested that they preferentially utilize lipids for energy whereas $IFABP^{-/-}$ mice have higher RERs, indicating preferential oxidation of carbohydrates for energy [16]. Overall, the disparate phenotypes of the $LFABP^{-/-}$ and $IFABP^{-/-}$ mice in response to high-fat feeding strongly suggest that these proteins play distinct roles in the intestine.

Interestingly, and in keeping with prior reports, neither LFABP$^{-/-}$ nor IFABP$^{-/-}$ mice showed evidence of overt lipid malabsorption on a HFD [16–18]. Nevertheless, despite the normal fecal fat content in IFABP$^{-/-}$ and LFABP$^{-/-}$ mice, we recently found that there are alterations in the quantity of feces excreted in both strains. LFABP$^{-/-}$ mice have lower fecal output per day, normalized to the amount of food consumed [19], while IFABP$^{-/-}$ mice have an opposite phenotype and display a higher fecal amount/gram of food consumed relative to WT mice [20].

Therefore, to further understand the unique and overlapping functions of these proteins in the intestine, and to interrogate their role in dietary lipid uptake, we generated mice that do not express either LFABP or IFABP. The results strongly support largely unique functional roles for these two proteins, and, unexpectedly, also demonstrate that they are not essential for the net intestinal uptake of dietary fat.

2. Experimental procedures

2.1. Animals and diets

LFABP$^{-/-}$ mice and IFABP$^{-/-}$ mice, and WT C57BL/6 J controls, were used as previously described [15,16,20,21]. LFABP and IFABP-double knockouts (DKO) were generated by breeding LFABP$^{-/-}$ and IFABP$^{-/-}$ mice, of which offspring were identified by DNA genotyping, immunoblotting and qPCR to verify simultaneous ablation of the two proteins in the intestine and LFABP in the liver (Fig. 1). The DKO mice were phenotypically normal and did not display any overt differences in breeding or litter sizes.

Mice were maintained on a 12-hour light/dark cycle and allowed ad libitum access to standard rodent chow (Purina Laboratory Rodent Diet 5015). At 2 months of age, male WT, IFABP$^{-/-}$, LFABP$^{-/-}$, and DKO mice were housed 2–3 per cage and fed one of the following diets for 12 weeks: a low fat diet (LFD) containing 10 kcal% fat or a 45 kcal% fat diet with high saturated fat (HSF) diet. Product numbers are D10080401 and D10080402 respectively (Research Diets, Inc., New Brunswick, NJ) and the compositions have been reported previously [16].

Body weights (BW) were measured weekly. At the end of the experiment, the mice were fasted for 16 h and anesthetized with ketamine/xylazine/acepromazine (80:100:150 mg/kg, intraperitoneally, respectively), prior to collection of blood and tissues. Rutgers University Animal Care and Use Committee approved all animal experiments.

2.2. Genotyping and immunoblotting to verify absence of IFABP and LFABP in DKO mice

Genotyping was performed as described previously [15]. Briefly, a 0.5 cm tail biopsy is incubated overnight at 37 °C in lysis buffer (0.3 M sodium acetate, 10 mM Tris-HCl pH 7.9, 1 mM EDTA, 1 % SDS, 0.2 mg/mL proteinase K). The following morning, the crude tail lysate is cooled on ice and the precipitate is pelleted by centrifugation in a pre-cooled microfuge at maximum speed. 100 μL of the clear supernatant is heated for 15 min at 95 °C to obtain a heat-inactivated cleared tail lysate.

LFABP genotyping was performed as described by Martin et al. [22]. PCR was performed with primers to amplify 123 base pairs of exon 2 of the WT allele (5′-CAAGGGGGTGTCAGAAATCGTGC and 5′-CCAGTCATGGTCTCCAGTTCGCA), or primers to amplify 227 base pairs of a sequence specific to the knockout (neomycin resistance marker: 5′-AAGAGCTTGGCGGCGAATGGand 5′-TGGCCATTTGTGGCTGTGCTC), 10× PCR buffer (SIGMA-buffer for REDTaq), dNTPs, REDTaqpolymerase (Sigma-Aldrich), and the heat-inactivated cleared tail lysate in a final volume of 25 μL. For IFABP genotyping, PCR was performed with primers to amply 804 base pairs of the WT allele (5′-TGTACACCACCATGGTTTGC-3′), or 208 base pairs of the KO sequence (5′-TGTGGAATGTGTGTGCGAGG-3′) as described by Vassileva et al. [23]. The primers were added to SYBR Green SuperMix (Bio-Rad) for a 20 μL reaction. 10 μL of the PCR reaction product was loaded directly onto a 2 % agarose gel and separated electrophoretically.

Western blotting of mucosa and liver was performed as described previously [15] to confirm ablation of IFABP and LFABP in intestinal mucosa and of LFABP in the liver. Results shown in Fig. 1 confirm the absence of both LFABP and IFABP.

2.3. Body composition, energy expenditure, and activity

Fat mass (FM) and lean body mass (LBM) measurements were taken by MRI (Echo Medical Systems, LLC., Houston, TX) as described previously [16]. Energy expenditure and activity were assessed using the Oxymax system (Columbus Instruments, Columbus, OH). Mice were placed individually in an indirect calorimetry chamber for a total of 48 h, which includes a 24-h period for adaptation prior to measurements [16].

2.4. Food intake and meal pattern analysis

Food consumption was measured using a BioDAQ food intake monitoring system (Research Diets, Inc., New Brunswick, NJ) with 16 cages. Eight-week-old male mice were individually housed in standard caging with continuous access to the HFD. Food intake measurements are recorded once per second. When the mouse is eating, the weight of the food hopper is unsteady. This is the start of a “bout”. The bout ends when the mouse stops eating and moves away from the food hopper. A “meal” is made up of a series of bouts within a determined time period and meal amounts. If the food hopper is not disturbed for a period, then the meal has ended and is counted. We defined the inter-meal interval as 10 min and a minimum meal amount of 0.02 g, as previously described [24]. The BioDAQ software (version 2.3.07) allows for measurements of cumulative intake, meal grams, number of meals, and the percent of time in meals.

2.5. Preparation of tissues and plasma

At sacrifice, blood was drawn and glucose (Accu-chek, Hoffmann-La Roche) and TG levels (Cardiochek, Polymer Technology Systems, Inc.) were measured. Plasma was extracted after centrifugation for 6 min at 4000 rpm and stored at −80 °C. Livers and inguinal, perirenal, and epididymal fat pads were removed, immediately placed on dry ice, and subsequently stored at −80 °C for further analysis. The intestine from stomach to cecum was removed and

measured lengthwise, rinsed with 60 mL ice-cold 0.1 M NaCl, opened longitudinally and mucosa scraped with a glass microscope slide into tared tubes in dry ice.

2.6. Plasma analyses

At time of sacrifice, plasma was collected and stored at −80 °C for further analyses as noted above. ELISA kits were used to measure plasma leptin, adiponectin, and insulin (Millipore). Plasma total cholesterol, TG, and FA levels were also analyzed (Wako Diagnostics, Inc.). Beta-hydroxybutyrate (BHB) levels were measured using Cardiochek (Polymer Technology Systems, Inc. Zionsville, IN). Adiponectin and leptin indices [25] were calculated as the plasma adiponectin or leptin levels divided by the total FM determined by MRI. Homeostatic Model Assessment (HOMA-IR) was determined using fasting glucose (mg/dl) × fasting insulin (μU/mL)/405 [26].

2.7. Oral glucose and insulin tolerance tests

During week 11 of high-fat feeding, mice were fasted for 6 h in preparation for an oral glucose tolerance test (OGTT). Time 0 blood was taken from conscious mice via the tail vein using 10 μL of whole blood with an Accu-Chek instrument (Roche Diagnostics, Inc. Basel, Switzerland). Immediately after the blood was taken for $t = 0$, the mice were orally gavaged with 2 g/kg BW of glucose. Blood was taken at $t = 30$, 60, 90, and 120 min. For insulin tolerance tests (ITT), mice were fasted for 6 h. Blood was taken at time 0 and injections of 0.75 U of insulin were given intraperitoneally. Blood was taken at t = 30, 60, 90, and 120 min.

2.8. Oral fat tolerance tests

After 3 months of high-fat feeding, mice were fasted for 24 h in preparation for an oral fat tolerance test (OFTT). Time 0 blood was taken from conscious mice via the tail vein and then an intraperitoneal injection of Tyloxapol (500 mg/kg BW) was administered to prevent lipoprotein TG uptake via inhibition of lipoprotein lipase. After 30 min, an orogastric gavage of 300 μL of olive oil was given. Blood was taken at $t = 1$, 2, 3, and 4 h. Blood TG levels were measured using 15 μL of whole blood with a Cardiochek instrument (Polymer Technology Systems, Inc. Zionsville, IN).

2.9. Fecal lipid content

Feces were collected from the cages after 4 weeks of feeding during the 12 week period and then dried overnight at 60 °C and weighed. 0.5 g (dry weight) was dissolved in water overnight and lipid extracted using the Folch method [27]. The extracted lipids in 2:1 chloroform:methanol were placed in pre-weighed glass tubes and dried down completely under a nitrogen stream. Tubes were weighed again to determine recovered lipid. The weight of the extract was divided by original weight of the feces to determine percent of lipid in the feces.

2.10. Intestinal lipid uptake localization

Mice were fasted for 5.5 h and orally gavaged with 8uCi [^{3}H] TG in 300 μL olive oil. After 1.5 h, mice were anesthetized with ketamine/xylazine/acepromazine (80:100:150 mg/kg,

intraperitoneally, respectively). The intestines were removed from the stomach to the cecum and cut into 2 cm sections from the proximal to the distal end and placed into individual vials. The vials were digested overnight in 750 μL 1 M NaOH at 65 °C. The radioactivity was measured in a scintillation counter the next day after 125 μL HCl was added, to determine the location of lipid uptake along the proximal to distal axis of the small intestine.

2.11. Intestinal transit time

Intestinal transit time measurements were performed between week 11 and 12 of the HF feeding period. Prior to the start of the experiment, mice were individually caged. After 2 h of acclimation, mice were gavaged with 250 μL of 6 % carmine red and 0.5 % methylcellulose (Sigma-Aldrich, St. Louis, MO) in PBS. After the oral gavage, the cages were checked every 10 min and the time of appearance of the first red fecal pellet was recorded [28,29].

2.12. Quantitative RT-PCR for mRNA expression analysis

The protocol for mRNA acquisition and analysis was adapted from Chon et al. [30]. Briefly, tissues were homogenized in 4 M guanidiniumthiocyanate, 25 mM sodium citrate, 0.1 M β-mercaptoethanol using several strokes of a Polytron. Total RNA was further purified by phenol extraction and the RNeasy cleanup kit (Qiagen, Valencia, CA) along with DNase treatment to minimize genomic DNA contamination. Reverse transcription was performed using 1 μg of RNA, random primers, an RNase inhibitor, and reverse transcriptase (Promega Madison, WI) in a total volume of 25 μL. Primer sequences were obtained from Primer Bank (Harvard Medical School QPCR primer data base). The efficiency of PCR amplifications was analyzed for all primers to confirm similar amplification efficiency. Real time PCR reactions were performed in triplicate using an Applied Biosystems 7300 instrument. Each reaction contained 80 ng cDNA, 250 nM of each primer, and 12.5 μL of SYBR Green Master Mix (Applied Biosystems, Foster City, CA) in a total volume of 25 μL. Relative quantification of mRNA expression was calculated using the comparative Ct method normalized to β-actin.

2.13. Statistical analysis

Data are presented as mean ± SD unless otherwise indicated. Statistical comparisons for body weights were made by two-way repeated measures ANOVA (genotype × time). Other comparisons were either made by one-way ANOVA followed by Tukey's post hoc test, or by Student's *t*-test vs WT, as indicated. Results were considered significant at $p < 0.05$.

3. Results

3.1. Effects of simultaneous ablation of LFABP and IFABP on BW and body composition

In agreement with our previous findings [16,20], IFABP$^{-/-}$ mice fed the LFD had similar BW relative to WT over the 12-week study, but HFD feeding resulted in lower BW and net weight gain relative to WT (p <0.05) (Fig. 2A, B, and C). Baseline FM of IFABP$^{-/-}$ mice was similar to WT, but LBM was slightly lower ($p < 0.05$) (Fig. 2D). IFABP$^{-/-}$ mice have similar body compositions relative to WT when fed LFD, but have reduced FM and a higher LBM relative to WT when fed HFD ($p < 0.05$) (Fig. 2E, F).

In contrast, LFABP$^{-/-}$ mice had similar BW relative to WT on LFD, but higher BWs and net weight gain after 12 weeks of HFD feeding ($p < 0.05$) (Fig. 2A, B, C) as observed previously [16]. The baseline body compositions of LFABP$^{-/-}$ mice were not different from WT, however, LFABP$^{-/-}$ mice had greater adiposity ($p < 0.05$) compared to WT when fed LFD and HFD, without changes in LBM (Fig. 2D, E), as observed previously [16].

Our previous results demonstrated that the IFABP$^{-/-}$ and LFABP$^{-/-}$ mice have opposite phenotypes in response to high-fat feeding, hence we were interested in the effects of simultaneous ablation of both enterocyte FABPs in response to the same dietary regimen [16]. We found that the whole-body phenotype of the DKO mice was intermediate between the LFABP$^{-/-}$ and IFABP$^{-/-}$ mice, and thus more similar to WT. Indeed, the DKO mice had similar BWs to WT when fed either the LFD or HFD during the 3 months of feeding (Fig. 2A, B). DKO mice also had similar net BW gain to the WT mice (Fig. 2C). Baseline FM and FM on LFD of DKO mice were higher than WT ($p < 0.05$), however the FM and LBM weights of DKO mice were similar to WT for the endpoint measurements (Fig. 2D, E, F). Overall, the effects of simultaneous ablation of IFABP and LFABP appeared to integrate the effects of the single gene ablations, and there was no predominant effect of ablation of either of the enterocyte FABPs in the absence of the other.

3.2. LFABP$^{-/-}$ and IFABP$^{-/-}$ mice have altered food intake

We measured meal patterns of mice fed the HFD using BioDaq instrumentation (Fig. 3), and observed that IFABP$^{-/-}$ mice ate less food than WT throughout the study (Fig. 3A). This is in agreement with our previous results, obtained using crude pellet weighing [16]. The present results also reveal that IFABP$^{-/-}$ mice eat fewer meals during the night compared to WT mice ($p < 0.05$) (Fig. 3C), and eat less food per day, particularly at night when the mice are active ($p < 0.05$) (Fig. 3D). In contrast to these results for the IFABP$^{-/-}$ mice, LFABP$^{-/-}$ mice tended to have greater cumulative food intake on the HFD relative to WT ($p = 0.07$) (Fig. 3A), particularly during the light period where they spent more time eating ($p < 0.05$), ate more meals ($p < 0.05$), and consumed more food ($p < 0.05$) (Fig. 3B–D).

Interestingly, and in keeping with many other analyses, we found that food intake of DKO mice was intermediate between the IFABP$^{-/-}$ and LFABP$^{-/-}$ mice. Food intake of DKO mice tended to be lower than LFABP$^{-/-}$, while higher than IFABP, and as such, were not different from WT. We did not find any differences in cumulative food intake, meal size, meal number, or time in meals for the DKO mice compared to the WT mice (Fig. 3A–D).

3.3. Ablation of IFABP and/or LFABP results in differences in markers of whole body energy metabolism

As previously found [16], fasting blood glucose, leptin, adiponectin levels, and fat pad weights of IFABP$^{-/-}$ mice were lower relative to WT mice when fed HFD ($p < 0.05$), but there were no changes in insulin, cholesterol, TG, or non-esterified fatty acid (NEFA), or plasma BHB (Table 1). Since we found much lower FM in IFABP$^{-/-}$ mice, leptin and adiponectin indices were used to normalize for adiposity; it was found that leptin levels per g FM of IFABP$^{-/-}$ mice were lower than WT, but adiponectin was not different. Total livers

weights of IFABP$^{-/-}$ mice were similar to WT and were also not different when normalized for BW.

LFABP$^{-/-}$ mice did not display differences in fasting blood glucose, insulin, cholesterol, TG, or adiponectin levels on HFD relative to WT mice (Table 1), in keeping with previous findings [16]. No changes were found in blood BHB levels relative to WT. Plasma NEFAs were higher in LFABP$^{-/-}$ mice when fed HFD and LFD ($p < 0.05$), possibly reflecting an increased rate of lipolysis during the fasted state. LFABP$^{-/-}$ mice on HFD had markedly higher leptin levels, which correspond to their increased adiposity compared to WT ($p < 0.05$) (Fig. 2E). Leptin levels expressed per g FM were higher than WT, while adiponectin levels were significantly lower when normalized for FM. As suggested by MRI measurements of FM (Fig. 2E), LFABP$^{-/-}$ mice had larger epididymal, perirenal, and inguinal fat pads when fed HFD ($p < 0.05$). Liver weights of LFABP$^{-/-}$ mice were lower than WT mice when expressed per g BW ($p < 0.05$).

DKO mice had blood glucose, insulin, cholesterol, TG, leptin, and adiponectin concentrations that were similar to WT mice fed LFD and HFD (Table 1). Like the LFABP$^{-/-}$ mice, plasma NEFA were higher in DKO mice when fed HFD ($p < 0.05$), and liver weights were lower than WT mice when expressed per g BW ($p < 0.05$). Blood BHB levels were lower for DKO mice relative to WT. Epididymal and perirenal fat pads were similar in mass to WT, although inguinal fat pads were larger ($p < 0.05$). Overall, metabolic markers for DKO mice were, in general, integrated between LFABP$^{-/-}$ and IFABP$^{-/-}$ mice, in that the phenotype did not appear to be more strongly influenced by ablation of one gene versus the other.

3.4. IFABP$^{-/-}$ mice have improved glucose metabolism during high-fat feeding

HFD-fed IFABP$^{-/-}$ mice displayed lower blood glucose levels at the 60, 90, and 120 min timepoints ($p < 0.05$), and a smaller area under the curve (Fig. 4) ($p < 0.05$), suggesting improved glucose tolerance relative to the other groups. Interestingly, despite their markedly increased adiposity, high-fat fed LFABP$^{-/-}$ mice were not different from WT mice (Fig. 4B). Glucose levels of DKO mice throughout the 2-hour time period were similar to LFABP$^{-/-}$ and WT mice (Fig. 4A, B).

Insulin tolerance tests were also performed on 6 h fasted mice fed HFD (Fig. 4C). In keeping with the findings from the OGTT, we observed that IFABP$^{-/-}$ mice had lower blood glucose following the insulin injections at $t = 30$, 60, and 90 min (Fig. 4C and D). Interestingly, DKO mice tended to follow IFABP$^{-/-}$, with lower blood glucose levels at t = 30 and 90 min, suggesting that they have somewhat improved insulin tolerance (Fig. 4C and D).

3.5. Ablation of IFABP and/or LFABP results in altered metabolic fuel source utilization and energy expenditure

We had previously observed differences in metabolic fuel source utilization between IFABP$^{-/-}$ and LFABP$^{-/-}$ mice [16]; hence we performed similar experiments using DKO mice fed LFD and HFD. In agreement with our previous results, IFABP$^{-/-}$ mice fed LFD were not different for VO_2 consumption and VCO_2 expiration, but they had higher VO_2 and VCO_2 than WT when fed HFD (Fig. 5A, B). LFABP$^{-/-}$ mice were opposite in that

they had lower VO_2 and VCO_2 during LFD and HFD feeding. As reported previously [16], the ratios of VCO_2/VO_2 for RER for IFABP$^{-/-}$ mice were higher than WT, suggesting that IFABP$^{-/-}$ have a preference for oxidation of carbohydrates as a fuel source ($p < 0.05$) (Fig. 5C). LFABP$^{-/-}$ mice, on the other hand, displayed lower RER on LFD and HFD compared to WT ($p < 0.05$) (Fig. 5A, B, C). The latter measurements are similar to our previous results which indicate that these mice preferentially oxidize lipids for energy [16]. No differences were noted for energy expenditure of IFABP$^{-/-}$ or LFABP$^{-/-}$ mice (Fig. 5D).

As noted above, our indirect calorimetry data have shown that the single knockout mice have divergent responses to high-fat feeding. In contrast to the phenotypes observed in the single KO mice, the DKO mice had lower VO_2 and VCO_2 levels relative to WT when fed the LFD ($p < 0.05$), but were similar during HFD feeding (Fig. 5A, B). The DKO mice had similar RER to WT mice when fed the LFD, but HFD feeding resulting in higher RER (Fig. 5C). This result suggests that the DKO mice are more similar to IFABP$^{-/-}$ mice and preferentially utilize carbohydrates as a fuel source and are dissimilar to the LFABP$^{-/-}$ mice which primarily metabolize lipid for energy. Like the two single knockouts, no differences were noted in energy expenditure in the DKO mice relative to WT (Fig. 5D).

3.6. LFABP ablation results in changes in spontaneous activity

We measured spontaneous activity of mice in the indirect calorimetry chambers when the lights are off (when the mice are most active), and when the lights are on (mice are least active) (Fig. 6), and did not observe any changes in activity for IFABP$^{-/-}$ mice relative to WT. LFABP$^{-/-}$ mice, on the other hand, and in keeping with our previous results [16], had increased 24 h X activity compared to WT mice after both LFD and HFD feeding ($p < 0.05$) (Fig. 6A, B), displaying higher ambulatory activity compared to WT during both dark and light photoperiods (Fig. 6C, D).

In contrast to LFABP$^{-/-}$ and IFABP$^{-/-}$ mice, the DKO mice tended to have somewhat lower spontaneous activity counts relative to WT for all measurements (Fig. 6A–F), which reached statistical significance for 24 h X activity and X ambulatory activity during HFD feeding ($p < 0.05$). This result was surprising given that we observed that the LFABP$^{-/-}$ mice had increased activity, while there were no changes observed for the IFABP$^{-/-}$ mice.

3.7. DKO mice show no alteration in fecal fat levels or intestinal FA uptake

In agreement with ours and others' previous results, no apparent changes in fat absorption, as indicated by fecal fat levels, were seen for either of the single knockout mice (Fig. 7A) [15–17]. Of great interest, DKO mice fed either LFD or even the HFD also showed no difference in fecal fat%, which likely indicates that there is no malabsorption of dietary lipid. These surprising results suggest that IFABP and LFABP are not required for the bulk uptake of dietary lipid by the intestine. Additionally, there was no changes in ^{3}H-labeled FA uptake along the proximal to distal axis of the small intestine of IFABP$^{-/-}$, LFABP$^{-/-}$ and DKO mice challenged with the 45 % Kcal HFD when compared to their WT control mice (Fig. 7B).

3.8. DKO mice do not exhibit alterations in chylomicron secretion rates

As we found previously [16], IFABP$^{-/-}$ mice displayed more rapid rates of TG secretion, while LFABP$^{-/-}$ were similar to WT mice. The DKO mice also exhibited no differences in TG secretion rates following an oral fat bolus, compared to WT (Fig. 7C and D).

3.9. Effects of IFABP and LFABP ablation on intestinal motility and fecal fat

Previously, we found that IFABP$^{-/-}$ mice had shorter intestinal transit time compared to the WT control mice [19,20], whereas the LFABP$^{-/-}$ mice showed an opposite phenotype with a longer intestinal transit time [19]. We observed a non-significant reduction in the intestinal transit time in the DKO mice, with results similar to those found in IFABP$^{-/-}$ mice, indicating increased intestinal motility (Fig. 8A). Additionally, we found that the DKO mice displayed no difference in daily fecal output compared to the WT control mice (Fig. 8B).

3.10. Effects of IFABP and LFABP ablation on expression of intestinal lipid binding proteins and lipid metabolic enzymes

We measured expression of genes involved in lipid metabolism and trafficking in the intestines of mice fed the HFD (Fig. 9). As found previously, we observed no compensation for IFABP or LFABP in the absence of the other protein in the single knockout mice [15]. In these single knockout as well as the DKO, there were also no changes in the very low mucosal levels of expression of the adipose (AFABP; FABP4), heart (HFABP; FABP3), or keratinocyte (KFABP; FABP5) FABPs (Fig. 9A). Indeed in the IFABP null, LFABP null, and DKO mice, we also found no changes in intestinal expression of Ileal lipid binding protein (ILBP; FABP6) (Fig. 9A), an FABP that is expressed in the distal region of the small intestine and is known for having higher affinity for bile acids than FA [31–33]. We also did not observe changes in expression of CD36, acyl CoA synthetase 5 (ACSL5), fatty acid transport protein 4 (FATP4), monoacylglycerol acyltransferase 2 (MGAT2), diacylglycerol acyl transferase 1 (DGAT1), monoacylglycerol lipase (MGL), micro-somal transport protein (MTP), or sterol carrier protein (SCP2). An increase in DGAT2 and scavenger receptor class B type 1 (SRB1) expression and a decrease in acyl-CoA binding protein 1 (ACBP1) expression were found in the LFABP$^{-/-}$ mice, in keeping with our prior results [16]. DGAT2 expression was elevated in the DKO mice, and ACBP1 was decreased in the DKO mice (Fig. 9B). No changes in the expression of TNF-alpha or IL-6 were found in any of the KO mice compared to the WT controls (Fig. 9C).

4. Discussion

Numerous differences in in vivo properties have suggested that LFABP and IFABP have distinct functions in the intestine [5–7,11–13]. To investigate their functional properties further, in the present studies we generated an LFABP/IFABP double knockout mouse. We found that DKO mice fed a HFD display BWs and composition that are in between those of LFABP$^{-/-}$ and IFABP$^{-/-}$ mice, which are opposite to each other [16]. The fact that we did not see a dominant effect in the DKO phenotype of either LFABP or IFABP, strongly supports the hypothesis that these proteins have different functions. The absence of compensatory upregulation of IFABP in intestinal mucosa in response to ablation of

LFABP, and vice versa [15,34], also suggests separable functions for these two proteins. Here, we also demonstrate that expression levels of other members of the FABP family were unchanged.

Lipid assimilation by the intestine is highly efficient, and it has long been assumed that the enterocyte FABPs play a role in net lipid uptake because they are abundantly expressed with maximal expression in the proximal intestine where lipid uptake is highest. Further, both enterocyte FABPs bind not only long chain FAs and MGs but also ECs, which play a role in food intake and intestinal motility [9,10] Expression of LFABP is also increased in response to high-fat feeding [35]. It was somewhat surprising, therefore, that LFABP$^{-/-}$ or IFABP$^{-/-}$ mice fed HFDs exhibit no signs of lipid malabsorption [16,17,23,36]. It was hypothesized that perhaps the presence of the other FABP was sufficient to accommodate even high levels of dietary fat ingestion. We tested this hypothesis directly by high-fat feeding of the DKO mice, expressing neither proximal intestinal FABP. Importantly, we found that DKO mice also do not show any change in fecal fat level relative to WT mice; weight gain in response to high-fat feeding was also similar to WT. Hence, we conclude that LFABP and IFABP do not, in fact, have an essential role in the net uptake of lipids into the intestine. This unexpected finding indicates that the high correlation between LFABP and IFABP levels and lipid absorption may be unrelated to bulk lipid processing; we propose, alternatively, that the intestinal FABP levels correlate with lipid assimilation because they function as sensors of dietary lipid.

Interestingly, despite the fact that there was no change in fecal fat per weight of feces, we found that IFABP$^{-/-}$ mice have a shorter intestinal transit time, indicative of faster gut motility. Indeed the IFABP null mice excrete more feces than WT mice [19,20], suggesting that there is less time available for nutrients to be absorbed, which may explain, in part, the leaner BW of IFABP$^{-/-}$ mice. The intestinal motility in LFABP$^{-/-}$ mice is opposite that of the IFABP$^{-/-}$ mice, with longer intestinal transit times and reduced fecal mass [19], indicative of slower gut motility which allows more time for nutrient absorption and might explain, in part, the heavier BW in LFABP$^{-/-}$ mice. Alterations in intestinal motility and food intake patterns may be attributed to differences in mucosal EC concentrations, and indeed LFABP$^{-/-}$ mice have a higher mucosal EC levels while IFABP$^{-/-}$ mice show a trend towards lower levels [16]. The relationship between gut motility and ECs levels is well established; higher concentrations of anandamide and 2-arachidonoylglycerol are associated with slower gut motility and greater food intake [37,38]. Intestinal transit time for the DKO mice was not significantly different than for WT mice, and the DKO mice did not have higher fecal output than the WT mice. In addition to lower EC concentrations, the faster intestinal motility in IFABP$^{-/-}$ mice may also be due to their short villi phenotype, allowing less hindrance of food passage [20]. Future studies will determine whether the DKO mice have intestinal morphology similar to the WT mice, as would be expected.

While we find that IFABP and LFABP are not limiting for lipid uptake by the intestine, it remains possible that these or other FABPs serve a regulatory role in FA uptake in other cell types. For example, uptake of radiolabeled FA into L-cell fibroblasts is increased when LFABP is overexpressed relative to controls [39]. Additionally, studies using primary hepatocytes of LFABP$^{-/-}$ mice have shown that FA uptake into liver is reduced relative to

WT [34,40], and hepatic uptake of FA is reduced in LFABP$^{-/-}$ mice relative to WT after 48 h of fasting, suggesting impairment of trafficking into liver [34]. We also found that functional reduction of AFABP in cultured adipocytes decreased FA uptake [41]. Thus, there is a growing understanding that each member of the FABP family has unique and potentially tissue-specific functions [42–45].

Lipids can enter the enterocyte via passive diffusion, though membrane transport proteins may also be involved because uptake is, in part, a saturable process [46]. We considered whether other proteins could be functioning to transport FA in the intestine in the dual absence of LFABP and IFABP. FATP4 and CD36 are enterocyte membrane proteins proposed to have a role in FA uptake [47,48], however, no changes in their expression were found in the LFABP$^{-/-}$, IFABP$^{-/-}$, or DKO mice. Since LFABP and IFABP are both expressed in the proximal small intestine, we investigated the possibility that net absorption of dietary lipid does not change owing to compensatory absorption in the distal small intestine. However, we found no differences in the localization of fat uptake into the intestine, nor where there changes in expression of other enterocyte proteins that can bind or acylate FA such as SCP, or ACSL5, although the latter showed a small decrease in expression in the DKO mice. On the contrary, there was a reduction in the expression of ACBP in both LFABP$^{-/-}$ and DKO mice.

A fundamental finding of these studies is that LFABP and IFABP are not required for efficient uptake of dietary lipid by the intestine. Given their simultaneous expression and high abundance, other roles in intestinal lipid assimilation must be considered. For example, by maintaining low intracellular unbound FA concentrations, they may act to prevent the cytotoxicity reported for high cellular long chain FA levels [49,50]. It is also possible that by regulating unbound concentrations of FAs, MGs, and other lipids inside the cell, the two enterocyte FABPs are acting as lipid sensors. In particular, binding of ECs by both enterocyte FABPs has been described [9,10], and both IFABP and LFABP null mice display altered MG and anandamide metabolism [16]. Thus, the enterocyte FABPs may be involved in signal transduction pathways secondary to regulation of FA and EC levels. Moreover, LFABP has been reported to traffic FA to PPARα, an important regulator of genes involved in lipid oxidation that is present in both the intestine and liver [51–54]. Recent studies have shown that ablation of LFABP results in attenuation of PPARα localization in the nucleus, thereby inhibiting its functionality [40,52]. We and others have shown that LFABP$^{-/-}$ mice have reduced intestinal and hepatic oxidation of FA relative to WT, hence LFABP appears to be involved in targeting FA towards oxidative pathways [15,16,40,55]. Therefore, LFABP may be acting as a nutrient sensor in response to high levels of FA, potentially playing a role in trafficking FA towards oxidative pathways via protein-protein interactions with PPARα. The hypothesis that IFABP and LFABP are involved in nutrient sensing in the intestine in response to feeding status is also supported by previous work using intestinal explants, which showed that both IFABP and LFABP are localized on the apical side of the enterocyte of fasted rats, but became localized throughout the cytoplasm in the fed state [56], suggesting that localization of these proteins is influenced by the availability of dietary FA.

We found several parameters where the DKO did not appear to integrate the observations in the single KO mice. Firstly, the DKO mice were found to have a higher RER in response to high-fat feeding relative to WT and are thus more similar to IFABP$^{-/-}$ mice, with a preference for carbohydrate oxidation. We speculate that fuel selection reflects fat stores, as the IFABP$^{-/-}$ mice have reduced adiposity, while LFABP$^{-/-}$ mice have greater amounts of adipose tissue lipids available for oxidation. The DKO mice do not have altered fat stores relative to WT but nevertheless appear to preferentially oxidize carbohydrate for energy. The DKO mice were also not intermediate between the two single FABP nulls with regard to physical activity. LFABP$^{-/-}$ mice have increased spontaneous activity and increased endurance while IFABP nulls are similar to WT [16,21], however we observed apparently lower spontaneous activity in the DKO mice. We recently found that LFABP$^{-/-}$ mice have improved endurance exercise capabilities secondary to increased intramuscular TG and glycogen stores and increased FA oxidation [21], thus we will investigate whether the DKO mice have altered stamina during an exercise test, and whether the decreased activity observed in DKO is accompanied by changes in muscle substrate availability and metabolism.

Using the pellet weighing method, we previously showed that LFABP$^{-/-}$ mice consume more calories, whereas IFABP$^{-/-}$ mice consume fewer calories than WT during high saturated fat feeding [16]. Here, we conducted in-depth meal pattern analysis using BioDaq instrumentation. We confirmed that IFABP$^{-/-}$ mice are consuming less total food, and now show that they consume fewer meals relative to WT mice, which correlates with their resistance to diet-induced obesity. The major effect on food intake occurred during the dark period, when mice are normally awake and eating. Interestingly, we found that the LFABP$^{-/-}$ mice eat more food than WT specifically when the lights are on, consuming double the amount of food during this photoperiod. The DKO mice, again, have a phenotype that is in between the IFABP$^{-/-}$ and LFABP$^{-/-}$ mice with food intakes that are more similar to WT. Mice are nocturnal and are more active during the dark cycle; hence, these data suggest that the LFABP$^{-/-}$ mice in particular may have alterations in circadian activity. Indeed, WT mice fed HFDs have been shown to have altered eating patterns shifting their food intake to the light photoperiod [57], which may contribute to their increased adiposity. Additionally, several transcription factors involved in the regulation of circadian genes have been identified in intestine, and the expression of genes for many proteins involved in intestinal lipid metabolism display diurnal variation, including IFABP and LFABP [57,58]. Additional studies will investigate alterations in expression of enterocyte clock genes, which may help elucidate the mechanisms underlying the apparent changes in circadian rhythms observed in the LFABP$^{-/-}$ mice.

In summary, the present studies demonstrate that simultaneous ablation of IFABP and LFABP results largely in an integration of the single knockout phenotypes, indicating that they are not functionally redundant and that one protein is not dominant over the other. Importantly, and contrary to long-held assumptions in the field, the results herein suggest that neither IFABP nor LFABP is critically required for net FA assimilation by the intestine. Rather, they appear to function as sensors of dietary fat, serving to signal the presence of lipid via as-yet largely unknown mechanisms, and thereby regulate whole body energy homeostasis.

Acknowledgments

The authors thank Dr. Luis Agellon (McGill University), Dr. Malcolm Watford (Rutgers University) and Dr. Loredana Quadro (Rutgers University) for helpful discussions. This work was supported by National Institutes of Health Grant DK-38389 and by funds from the New Jersey Agricultural Experiment Station (to J. S.).

Data availability

Data will be made available on request.

Abbreviations:

TG	triglyceride
MG	monoglyceride
FA	fatty acid
LFABP	Liver fatty acid binding protein
IFABP	Intestinal fatty acid binding protein
ECs	endocannabinoids
RER	respiratory exchange ratio
HFD	High-fat diet
WT	wild-type
DKO	double knockout
OGTT	oral glucose tolerance test
ITT	insulin tolerance test
OFTT	oral fat tolerance test
LFD	low-fat diet
FM	fat mass
LBM	lean body mass
BW	body weight
BHB	Beta-hydroxybutyrate
NEFA	non-esterified fatty acid
AFABP	adipocyte FABP
HFABP	heart FABP
KFABP	keratinocyte FABP

ILBP ileal lipid binding protein

References

[1]. Tso P, Crissinger K, Vol, in: Stipanuk MH (Ed.), Biochemical, Physiological, Molecular Aspects of Human Nutrition, Second, Elsevier, St. Louis, MO, 2006, pp. 151–167.

[2]. Furuhashi M, Hotamisligil GS, Fatty acid-binding proteins: role in metabolic diseases and potential as drug targets, Nat. Rev. Drug Discov 7 (2008) 489–503, 10.1038/nrd2589. [PubMed: 18511927]

[3]. Gordon JI, Elshourbagy N, Lowe JB, Liao WS, Alpers DH, Taylor JM, Tissue specific expression and developmental regulation of two genes coding for rat fatty acid binding proteins, J. Biol. Chem 260 (1985) 1995–1998. [PubMed: 2579065]

[4]. Levy E, Ménard D, Delvin E, Montoudis A, Beaulieu JF, Mailhot G, Dubé N, Sinnett D, Seidman E, Bendayan M, Localization, function and regulation of the two intestinal fatty acid-binding protein types, Histochem. Cell Biol 132 (2009) 351–367, 10.1007/s00418-009-0608-y. [PubMed: 19499240]

[5]. Lagakos WS, Guan X, Ho SY, Sawicki LR, Corsico B, Kodukula S, Murota K, Stark RE, Storch J, Liver fatty acid-binding protein binds monoacylglycerol in vitro and in mouse liver cytosol, J. Biol. Chem 288 (2013) 19805–19815, 10.1074/jbc.M113.473579. [PubMed: 23658011]

[6]. Wolfrum C, Börchers T, Sacchettini JC, Spener F, Binding of fatty acids and peroxisome proliferators to orthologous fatty acid binding proteins from human, murine, and bovine liver, Biochemistry 39 (2000) 1469–1474, 10.1021/bi991638u. [PubMed: 10684629]

[7]. Richieri GV, Ogata RT, Kleinfeld AM, Equilibrium constants for the binding of fatty acids with fatty acid-binding proteins from adipocyte, intestine, heart, and liver measured with the fluorescent probe ADIFAB, J. Biol. Chem 269 (1994) 23918–23930. [PubMed: 7929039]

[8]. Richieri GV, Ogata RT, Zimmerman AW, Veerkamp JH, Kleinfeld AM, Fatty acid binding proteins from different tissues show distinct patterns of fatty acid interactions, Biochemistry 39 (2000) 7197–7204, 10.1021/bi000314z. [PubMed: 10852718]

[9]. Huang H, McIntosh AL, Martin GG, Landrock D, Chung S, Landrock KK, Dangott LJ, Li S, Kier AB, Schroeder F, FABP1: a novel hepatic endocannabinoid and cannabinoid binding protein, Biochemistry 55 (2016) 5243–5255, 10.1021/acs.biochem.6b00446. [PubMed: 27552286]

[10]. Lai MP, Katz FS, Bernard C, Storch J, Stark RE, Two fatty acid-binding proteins expressed in the intestine interact differently with endocannabinoids, Protein Sci. 29 (2020) 1606–1617, 10.1002/pro.3875. [PubMed: 32298508]

[11]. Corsico B, Cistola DP, Frieden C, Storch J, The helical domain of intestinal fatty acid binding protein is critical for collisional transfer of fatty acids to phospholipid membranes, Proc. Natl. Acad. Sci. U. S. A 95 (1998) 12174–12178, 10.1073/pnas.95.21.12174. [PubMed: 9770459]

[12]. Falomir-Lockhart LJ, Franchini GR, Guerbi MX, Storch J, Córsico B, Interaction of enterocyte FABPs with phospholipid membranes: clues for specific physiological roles, Biochim. Biophys. Acta 1811 (2011) 452–459, 10.1016/j.bbalip.2011.04.005. [PubMed: 21539932]

[13]. Hsu KT, Storch J, Fatty acid transfer from liver and intestinal fatty acid-binding proteins to membranes occurs by different mechanisms, J. Biol. Chem 271 (1996) 13317–13323, 10.1074/jbc.271.23.13317. [PubMed: 8662836]

[14]. Agellon LB, Drozdowski L, Li L, Iordache C, Luong L, Clandinin MT, Uwiera RRE, Toth MJ, Thomson ABR, Loss of intestinal fatty acid binding protein increases the susceptibility of male mice to high fat diet-induced fatty liver, Biochim. Biophys. Acta Mol. Cell Biol. Lipids 1771 (2007) 1283–1288, 10.1016/j.bbalip.2007.08.004.

[15]. Lagakos WS, Gajda AM, Agellon L, Binas B, Choi V, Mandap B, Russnak T, Zhou YX, Storch J, Different functions of intestinal and liver-type fatty acid-binding proteins in intestine and in whole body energy homeostasis, Am. J. Physiol. Gastrointest. Liver Physiol 300 (2011) G803–G814, 10.1152/ajpgi.00229.2010. [PubMed: 21350192]

[16]. Gajda AM, Zhou YX, Agellon LB, Fried SK, Kodukula S, Fortson W, Patel K, Storch J, Direct comparison of mice null for liver or intestinal fatty acid-binding proteins reveals highly

divergent phenotypic responses to high fat feeding, J. Biol. Chem 288 (2013) 30330–30344, 10.1074/jbc.M113.501676. [PubMed: 23990461]

[17]. Newberry EP, Kennedy SM, Xie Y, Luo J, Davidson NO, Diet-induced alterations in intestinal and extrahepatic lipid metabolism in liver fatty acid binding protein knockout mice, Mol. Cell. Biochem 326 (2009) 79–86, 10.1007/s11010-008-0002-4. [PubMed: 19116776]

[18]. Newberry EP, Xie Y, Kennedy SM, Luo J, Davidson NO, Protection against Western diet-induced obesity and hepatic steatosis in liver fatty acid-binding protein knockout mice, Hepatology (Baltimore, Md.) 44 (2006) 1191–1205, 10.1002/hep.21369.

[19]. Wu G, Tawfeeq HR, Lackey AI, Zhou Y, Sifnakis Z, Zacharisen SM, Xu H, Doran JM, Sampath H, Zhao L, et al. , Gut microbiota and phenotypic changes induced by ablation of liver- and intestinal-type fatty acid-binding proteins, Nutrients 14 (2022), 10.3390/nu14091762.

[20]. Lackey AI, Chen T, Zhou YX, Bottasso Arias NM, Doran JM, Zacharisen SM, Gajda AM, Jonsson WO, Córsico B, Anthony TG, Mechanisms underlying reduced weight gain in intestinal fatty acid-binding protein (IFABP) null mice, Am. J. Physiol. Gastrointest. Liver Physiol 318 (2020) G518–g530, 10.1152/ajpgi.00120.2019. [PubMed: 31905021]

[21]. Xu H, Gajda AM, Zhou YX, Panetta C, Sifnakis Z, Fatima A, Henderson GC, Storch J, Muscle metabolic reprogramming underlies the resistance of liver fatty acid-binding protein (LFABP)-null mice to high-fat feeding-induced decline in exercise capacity, J. Biol. Chem 294 (2019) 15358–15372, 10.1074/jbc.RA118.006684. [PubMed: 31451493]

[22]. Martin GG, Danneberg H, Kumar LS, Atshaves BP, Erol E, Bader M, Schroeder F, Binas B, Decreased liver fatty acid binding capacity and altered liver lipid distribution in mice lacking the liver fatty acid-binding protein gene, J. Biol. Chem 278 (2003) 21429–21438, 10.1074/jbc.M300287200. [PubMed: 12670956]

[23]. Vassileva G, Huwyler L, Poirier K, Agellon LB, Toth MJ, The intestinal fatty acid binding protein is not essential for dietary fat absorption in mice, FASEB J. 14 (2000) 2040–2046, 10.1096/fj.99-0959com. [PubMed: 11023988]

[24]. Dill MJ, Shaw J, Cramer J, Sindelar DK, 5-HT1A receptor antagonists reduce food intake and body weight by reducing total meals with no conditioned taste aversion, Pharmacol. Biochem. Behav 112 (2013) 1–8, 10.1016/j.pbb.2013.09.003. [PubMed: 24064183]

[25]. Nishiumi S, Bessyo H, Kubo M, Aoki Y, Tanaka A, Yoshida K, Ashida H, Green and black tea suppress hyperglycemia and insulin resistance by retaining the expression of glucose transporter 4 in muscle of high-fat diet-fed C57BL/6J mice, J. Agric. Food Chem 58 (2010) 12916–12923, 10.1021/jf102840w. [PubMed: 21105694]

[26]. Matthews DR, Hosker JP, Rudenski AS, Naylor BA, Treacher DF, Turner RC, Homeostasis model assessment: insulin resistance and β-cell function from fasting plasma glucose and insulin concentrations in man, Diabetologia 28 (1985) 412–419, 10.1007/BF00280883. [PubMed: 3899825]

[27]. Folch J, Lees M, Sloane Stanley GHA, Simple method for the isolation and purification of total lipides from animal tissues, J. Biol. Chem 226 (1957) 497–509. [PubMed: 13428781]

[28]. Kelly JR, Borre Y, O.B. C, E. Patterson, S. El Aidy, J. Deane, P.J. Kennedy, S. Beers, K. Scott, G. Moloney, Transferring the blues: depression-associated gut microbiota induces neurobehavioural changes in the rat, J. Psychiatr. Res 82 (2016) 109–118, 10.1016/j.jpsychires.2016.07.019. [PubMed: 27491067]

[29]. Nagakura Y, Ito H, Kiso T, Naitoh Y, Miyata K, The selective 5-hydroxytrypta-mine (5-HT)4-receptor agonist RS67506 enhances lower intestinal propulsion in mice, Jpn. J. Pharmacol 74 (1997) 209–212, 10.1254/jjp.74.209. [PubMed: 9243330]

[30]. Chon S-H, Zhou YX, Dixon JL, Storch J, Intestinal monoacylglycerol metabolism: developmental and nutritional regulation of monoacylglycerol lipase and monoacylglycerol acyltransferase*, J. Biol. Chem 282 (2007) 33346–33357, 10.1074/jbc.M706994200. [PubMed: 17848545]

[31]. Agellon LB, Toth MJ, Thomson AB, Intracellular lipid binding proteins of the small intestine, Mol. Cell. Biochem 239 (2002) 79–82. [PubMed: 12479571]

[32]. Gong YZ, Everett ET, Schwartz DA, Norris JS, Wilson FA, Molecular cloning, tissue distribution, and expression of a 14-kDa bile acid-binding protein from rat ileal cytosol, Proc. Natl. Acad. Sci. U. S. A 91 (1994) 4741–4745, 10.1073/pnas.91.11.4741. [PubMed: 8197128]

[33]. Sacchettini JC, Hauft SM, Van Camp SL, Cistola DP, Gordon JI, Developmental and structural studies of an intracellular lipid binding protein expressed in the ileal epithelium, J. Biol. Chem 265 (1990) 19199–19207. [PubMed: 1699943]

[34]. Newberry EP, Xie Y, Kennedy S, Han X, Buhman KK, Luo J, Gross RW, Davidson NO, Decreased hepatic triglyceride accumulation and altered fatty acid uptake in mice with deletion of the liver fatty acid-binding protein gene, J. Biol. Chem 278 (2003) 51664–51672, 10.1074/jbc.M309377200. [PubMed: 14534295]

[35]. Storch J, Herr F, in: Nutritional Regulation of Fatty Acid Transport Protein Expression, 2001, pp. 101–130, 10.1201/9781420039108-6pp.

[36]. Newberry EP, Kennedy SM, Xie Y, Sternard BT, Luo J, Davidson NO, Diet-induced obesity and hepatic steatosis in L-Fabp/mice is abrogated with SF, but not PUFA, feeding and attenuated after cholesterol supplementation, Am. J. Physiol. Gastrointest. Liver Physiol 294 (2008) G307–G314, 10.1152/ajpgi.00377.2007. [PubMed: 18032478]

[37]. DiPatrizio NV, Endocannabinoids in the Gut, in: Cannabis and Cannabinoid Research 1, 2016, pp. 67–77, 10.1089/can.2016.0001.

[38]. Vianna CR, Donato J Jr., J. Rossi, M. Scott, K. Economides, L. Gautron, S. Pierpont, C.F. Elias, J.K. Elmquist, Cannabinoid receptor 1 in the vagus nerve is dispensable for body weight homeostasis but required for normal gastrointestinal motility, J. Neurosci. Off. J. Soc. Neurosci 32 (2012) 10331–10337, 10.1523/jneurosci.4507-11.2012.

[39]. Murphy EJ, Prows DR, Jefferson JR, Schroeder F, Liver fatty acid-binding protein expression in transfected fibroblasts stimulates fatty acid uptake and metabolism, Biochim. Biophys. Acta 1301 (1996) 191–198, 10.1016/0005-2760(96)00024-0. [PubMed: 8664328]

[40]. McIntosh AL, Atshaves BP, Hostetler HA, Huang H, Davis J, Lyuksyutova OI, Landrock D, Kier AB, Schroeder F, Liver type fatty acid binding protein (L-FABP) gene ablation reduces nuclear ligand distribution and peroxisome proliferator-activated receptor-alpha activity in cultured primary hepatocytes, Arch. Biochem. Biophys 485 (2009) 160–173, 10.1016/j.abb.2009.03.004. [PubMed: 19285478]

[41]. Shaughnessy S, Smith ER, Kodukula S, Storch J, Fried SK, Adipocyte metabolism in adipocyte fatty acid binding protein knockout mice (aP2−/−) after short-term high-fat feeding: functional compensation by the keratinocyte [correction of keritinocyte] fatty acid binding protein, Diabetes 49 (2000) 904–911, 10.2337/diabetes.49.6.904. %J Diabetes. [PubMed: 10866041]

[42]. Storch J, Corsico B, The emerging functions and mechanisms of mammalian fatty acid-binding proteins, Annu. Rev. Nutr 28 (2008) 73–95, 10.1146/annurev.nutr.27.061406.093710. [PubMed: 18435590]

[43]. Storch J, McDermott L, Structural and functional analysis of fatty acid-binding proteins, J. Lipid Res 50 (Suppl) (2009) S126–S131, 10.1194/jlr.R800084-JLR200. [PubMed: 19017610]

[44]. Storch J, Thumser AE, Tissue-specific functions in the fatty acid-binding protein family, J. Biol. Chem 285 (2010) 32679–32683, 10.1074/jbc.R110.135210. [PubMed: 20716527]

[45]. Xu H, Diolintzi A, Storch J, Fatty acid-binding proteins: functional understanding and diagnostic implications, Curr. Opin. Clin. Nutr. Metab. Care 22 (2019) 407–412, 10.1097/mco.0000000000000600. [PubMed: 31503024]

[46]. Murota K, Storch J, Uptake of micellar long-chain fatty acid and sn-2-monoacylglycerol into human intestinal Caco-2 cells exhibits characteristics of protein-mediated transport, J. Nutr 135 (2005) 1626–1630, 10.1093/jn/135.7.1626. [PubMed: 15987840]

[47]. Abumrad NA, Davidson NO, Role of the gut in lipid homeostasis, Physiol. Rev 92 (2012) 1061–1085, 10.1152/physrev.00019.2011. [PubMed: 22811425]

[48]. Niot I, Poirier H, Tran TTT, Besnard P, Intestinal absorption of long-chain fatty acids: evidence and uncertainties, Prog. Lipid Res 48 (2009) 101–115, 10.1016/j.plipres.2009.01.001. [PubMed: 19280719]

[49]. Kazantzis M, Stahl A, Fatty acid transport proteins, implications in physiology and disease, Biochim. Biophys. Acta 1821 (2012) 852–857, 10.1016/j.bbalip.2011.09.010. [PubMed: 21979150]

[50]. Listenberger LL, Ory DS, Schaffer JE, Palmitate-induced apoptosis can occur through a ceramide-independent pathway, J. Biol. Chem 276 (2001) 14890–14895, 10.1074/jbc.M010286200. [PubMed: 11278654]

[51]. Braissant O, Foufelle F, Scotto C, Dauça M, Wahli W, Differential expression of peroxisome proliferator-activated receptors (PPARs): tissue distribution of PPAR-alpha, -beta, and -gamma in the adult rat, Endocrinology 137 (1996) 354–366, 10.1210/endo.137.1.8536636. [PubMed: 8536636]

[52]. Hostetler HA, McIntosh AL, Atshaves BP, Storey SM, Payne HR, Kier AB, Schroeder F, L-FABP directly interacts with PPARalpha in cultured primary hepatocytes, J. Lipid Res 50 (2009) 1663–1675, 10.1194/jlr.M900058-JLR200. [PubMed: 19289416]

[53]. Huang H, Starodub O, McIntosh A, Atshaves BP, Woldegiorgis G, Kier AB, Schroeder F, Liver fatty acid-binding protein colocalizes with peroxisome proliferator activated receptor α and enhances ligand distribution to nuclei of living cells, Biochemistry 43 (2004) 2484–2500, 10.1021/bi0352318. [PubMed: 14992586]

[54]. Petrescu AD, Huang H, Martin GG, McIntosh AL, Storey SM, Landrock D, Kier AB, Schroeder F, Impact of L-FABP and glucose on polyunsaturated fatty acid induction of PPARα-regulated β-oxidative enzymes, Am. J. Physiol. Gastrointest. Liver Physiol 304 (2013) G241–G256, 10.1152/ajpgi.00334.2012. [PubMed: 23238934]

[55]. Erol E, Kumar LS, Cline GW, Shulman GI, Kelly DP, Binas B, Liver fatty acid binding protein is required for high rates of hepatic fatty acid oxidation but not for the action of PPARalpha in fasting mice, FASEB J. 18 (2004) 347–349, 10.1096/fj.03-0330fje. [PubMed: 14656998]

[56]. Alpers DH, Bass NM, Engle MJ, DeSchryver-Kecskemeti K, Intestinal fatty acid binding protein may favor differential apical fatty acid binding in the intestine, Biochim. Biophys. Acta 1483 (2000) 352–362, 10.1016/s1388-1981(99)00200-0. [PubMed: 10666570]

[57]. Kohsaka A, Laposky AD, Ramsey KM, Estrada C, Joshu C, Kobayashi Y, Turek FW, Bass J, High-fat diet disrupts behavioral and molecular circadian rhythms in mice, Cell Metab. 6 (2007) 414–421, 10.1016/j.cmet.2007.09.006. [PubMed: 17983587]

[58]. Glatz JF, Baerwaldt CC, Veerkamp JH, Kempen HJ, Diurnal variation of cytosolic fatty acid-binding protein content and of palmitate oxidation in rat liver and heart, J. Biol. Chem 259 (1984) 4295–4300, 10.1016/S0021-9258(17)43044-4. [PubMed: 6538567]

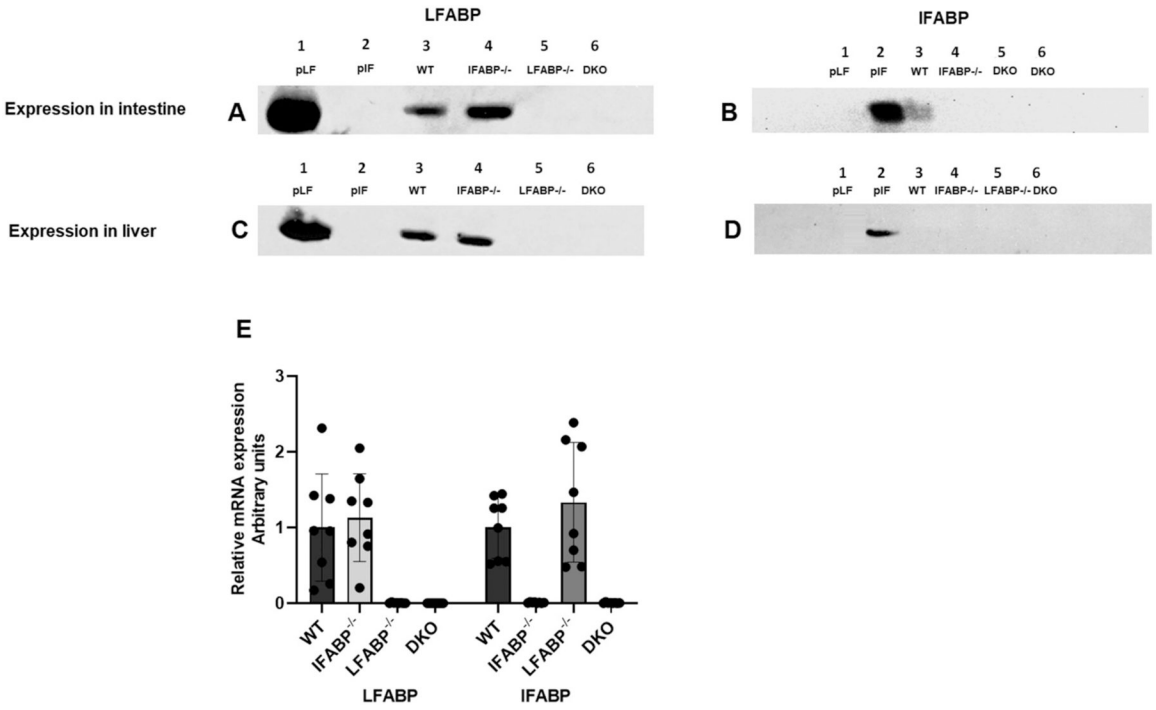

Fig. 1.

Verification of genotype by Immunoblotting. Representative images of Western blotting. A. Probing for LFABP in intestine: Lane 1, purified LFABP (pLF); Lane 2, purified IFABP (pIF); Lane 3, WT; Lane 4, IFABP$^{-/-}$; Lane 5, LFABP$^{-/-}$; Lane 6, DKO. B. Probing for IFABP in intestine: Lane 1, pLF; Lane 2, pIF; Lane 3, WT; Lane 4, IFABP$^{-/-}$; Lane 5 and Lane 6, DKO. C. Probing for LFABP in liver: Lane 1, pLF; Lane 2, pIF; Lane 3, WT; Lane 4, IFABP$^{-/-}$; Lane 5, LFABP$^{-/-}$; Lane 6, DKO. D. Probing for IFABP in liver: Lane 1, pLF; Lane 2, pIF; Lane 3, WT; Lane 4, IFABP$^{-/-}$; Lane 5, LFABP$^{-/-}$; Lane 6, DKO. E. Intestinal expression of LFABP and IFABP in WT, IFABP$^{-/-}$, LFABP$^{-/-}$ and DKO mice. n = 7–8 mice for each group.

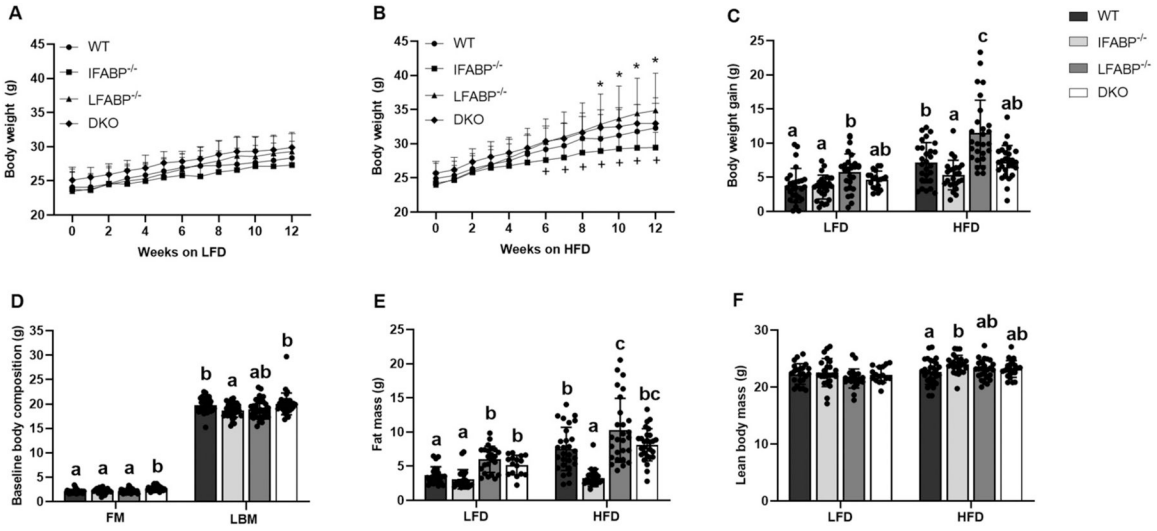

Fig. 2.

Body weight and composition for WT, IFABP$^{-/-}$, LFABP$^{-/-}$, and DKO mice after 12 weeks on a low-fat (LFD) or high saturated fat (HFD). A. Body weights on LFD (n = 18–29); B. Body weights on HFD (n = 27–30); C. Body weight gain (n = 19–29); D. Baseline body composition (n = 31–39); E. Fat mass (n = 16–28); F. Lean body mass (16–28). For figs. A–B, data are mean ± SD, analyzed using two way ANOVA using repeated measures with post hoc Tukey's test (genotype × time). For figs. C–F, data are mean ± SD, analyzed using one way ANOVA with a Tukey's post hoc test. Results with different letters within diet treatment are significantly different ($p < 0.05$).

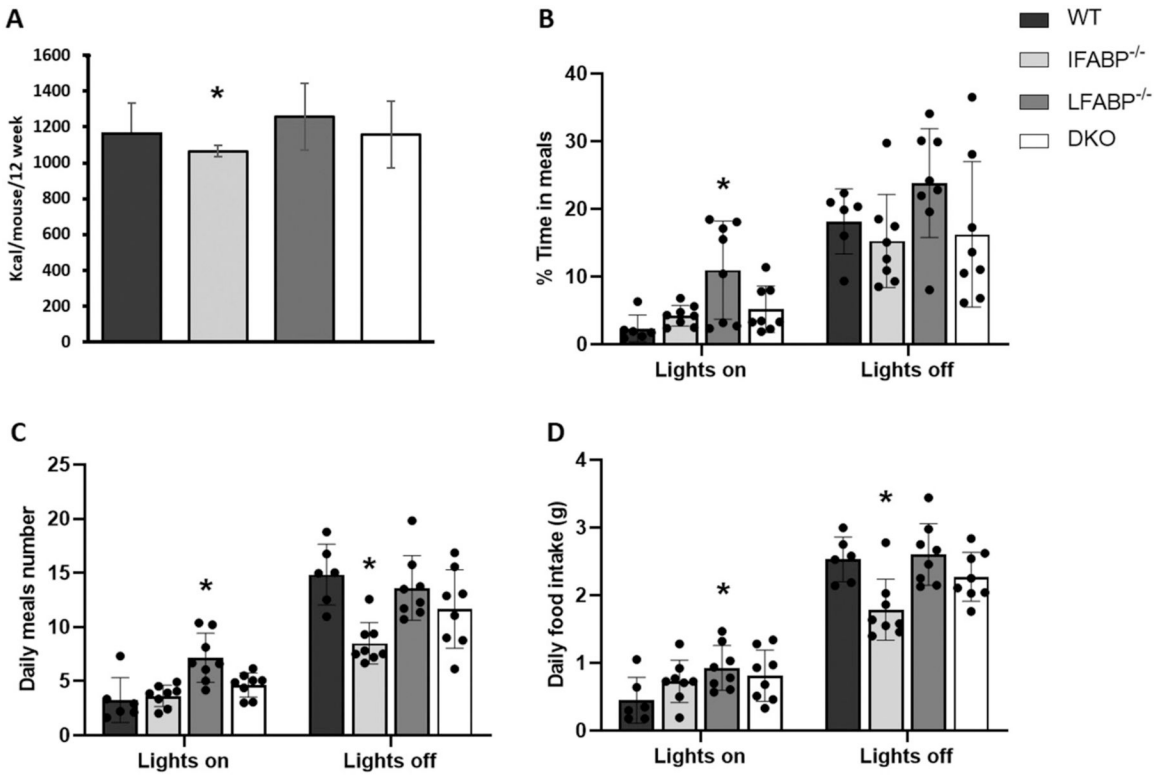

Fig. 3.

Meal pattern analysis for WT, IFABP$^{-/-}$, LFABP$^{-/-}$, and DKO mice fed high saturated fat diet. A. Cumulative intake (n = 4); B. % Time in meals; C. Daily meal number; D. Daily food intake. n = 6–8/group. Data are given as mean ± SD, analyzed using Student's t-test *p < 0.05 vs WT.

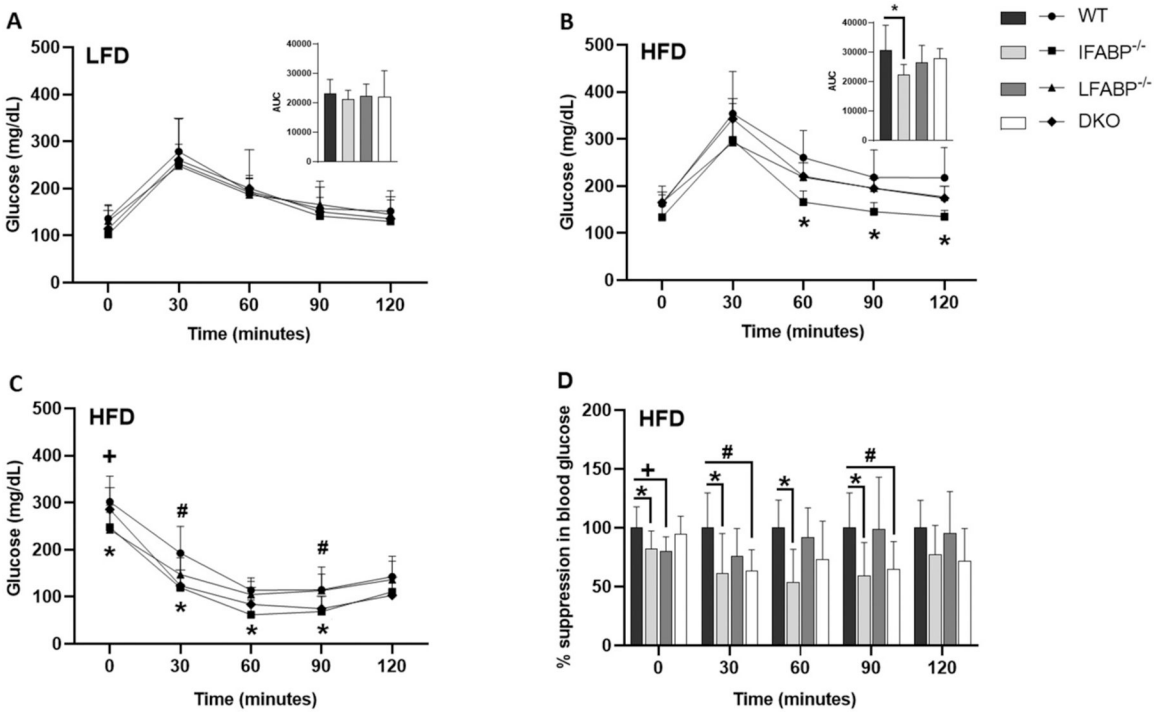

Fig. 4.

Oral glucose (OGTT) and insulin (ITT) tolerance tests for WT (●), IFABP$^{-/-}$ (■), LFABP$^{-/-}$ (▲), and DKO (◆) mice of mice fed a low-fat (LFD) or high saturated fat (HFD) diet. A. OGTT for LFD-fed mice; B. OGTT for HFD-fed mice; C. ITT for HFD-fed mice; D. % suppression in blood glucose over time. AUC, area under the curve. Data are mean ± SD, analyzed using Student's *t*-test. *$p < 0.05$ for IFABP$^{-/-}$ vs WT. $^{+}p < 0.05$ for LFABP$^{-/-}$ vs WT. $^{\#}p < 0.05$ for DKO vs WT. $n = 6–9$ for all groups.

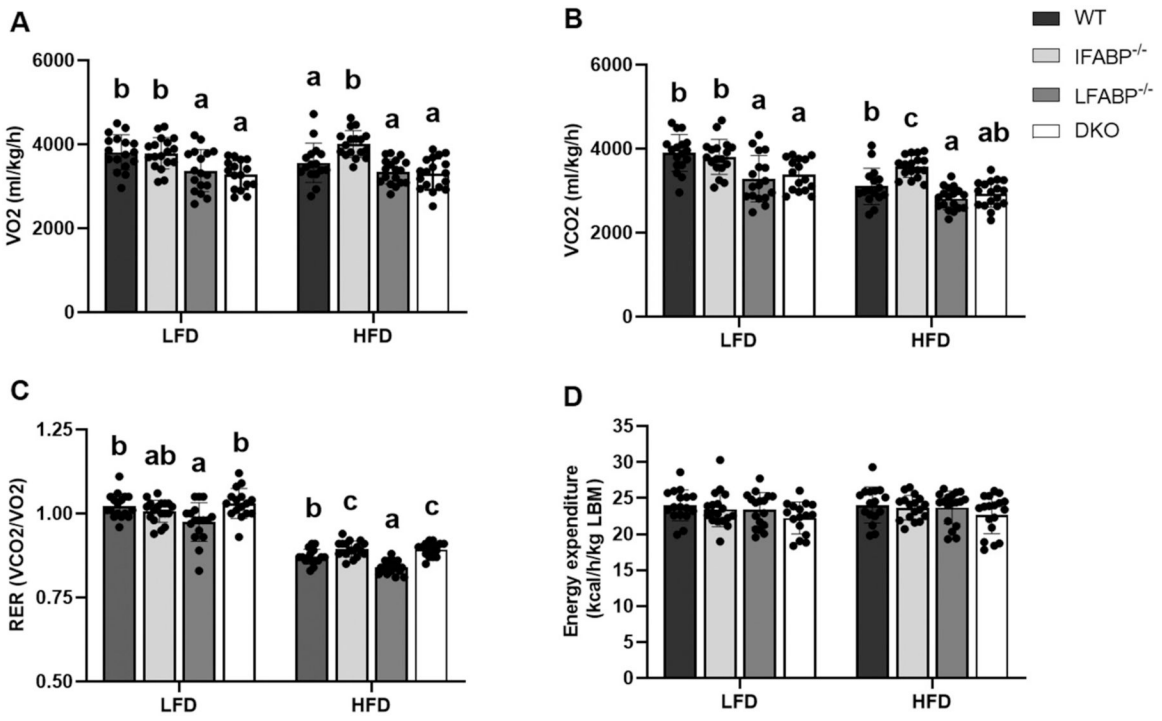

Fig. 5.

Indirect calorimetry for WT, IFABP$^{-/-}$, LFABP$^{-/-}$, and DKO mice fed a low-fat (LFD) or high saturated fat (HFD) diet. A. VO_2; B. VCO_2; C. Respiratory Exchange Ratio; D. Energy expenditure. Data presented as mean ± SD, analyzed using one-way ANOVA with Tukey's post hoc test. n = 16–18/group. Results with different letters within a dietary treatment are significantly different ($p < 0.05$).

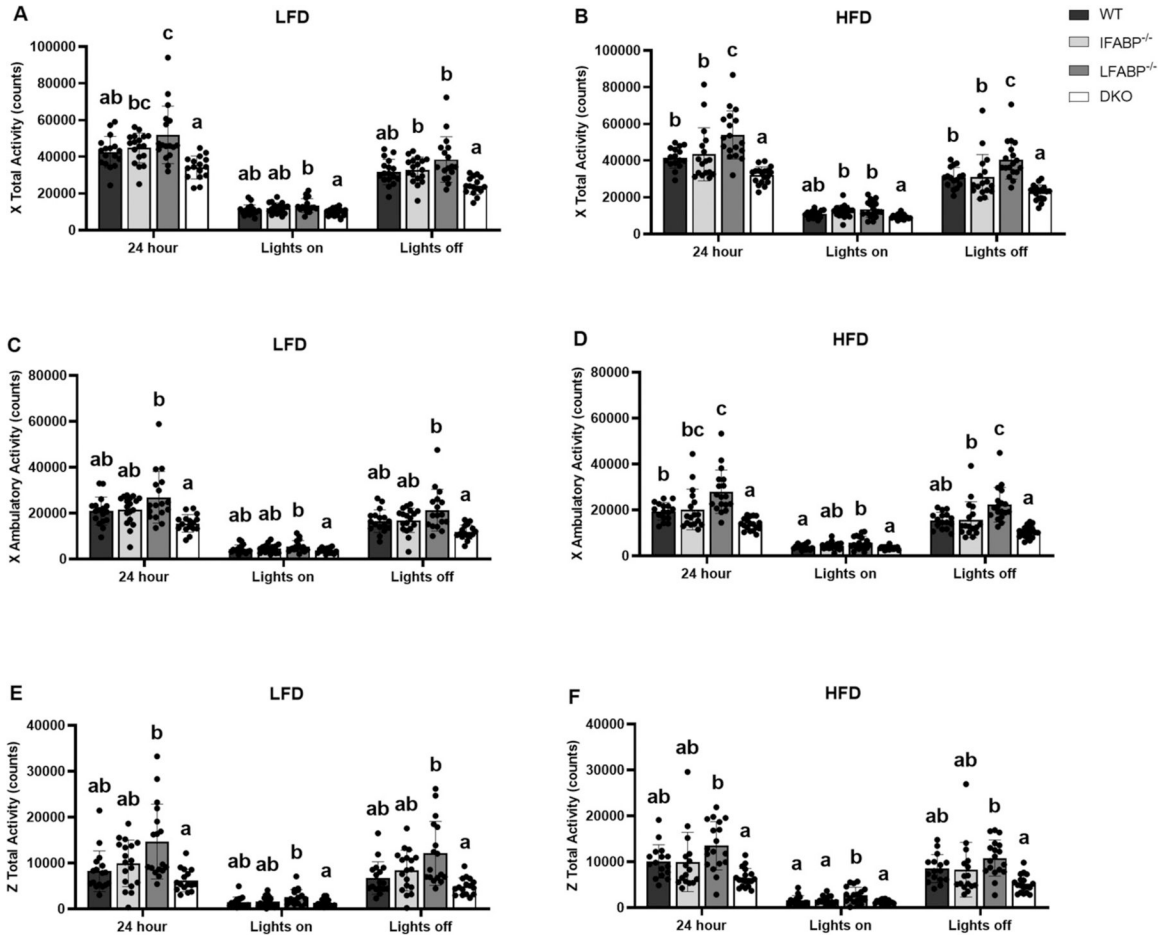

Fig. 6.

24-Hour activity of WT, IFABP$^{-/-}$, LFABP$^{-/-}$, and DKO mice fed low-fat (LFD) or a high saturated fat (HFD) diet. A. X Activity on LFD; B. X Activity on HFD; C. X ambulatory activity on LFD; D. X ambulatory activity on HFD; E. Z total activity on LFD; F. Z total activity on HFD. Data are mean ± SD, analyzed using one-way ANOVA with Tukey's post hoc test. n = 16–18/group. Results with different letters within a dietary treatment for the same time period are significantly different ($p < 0.05$).

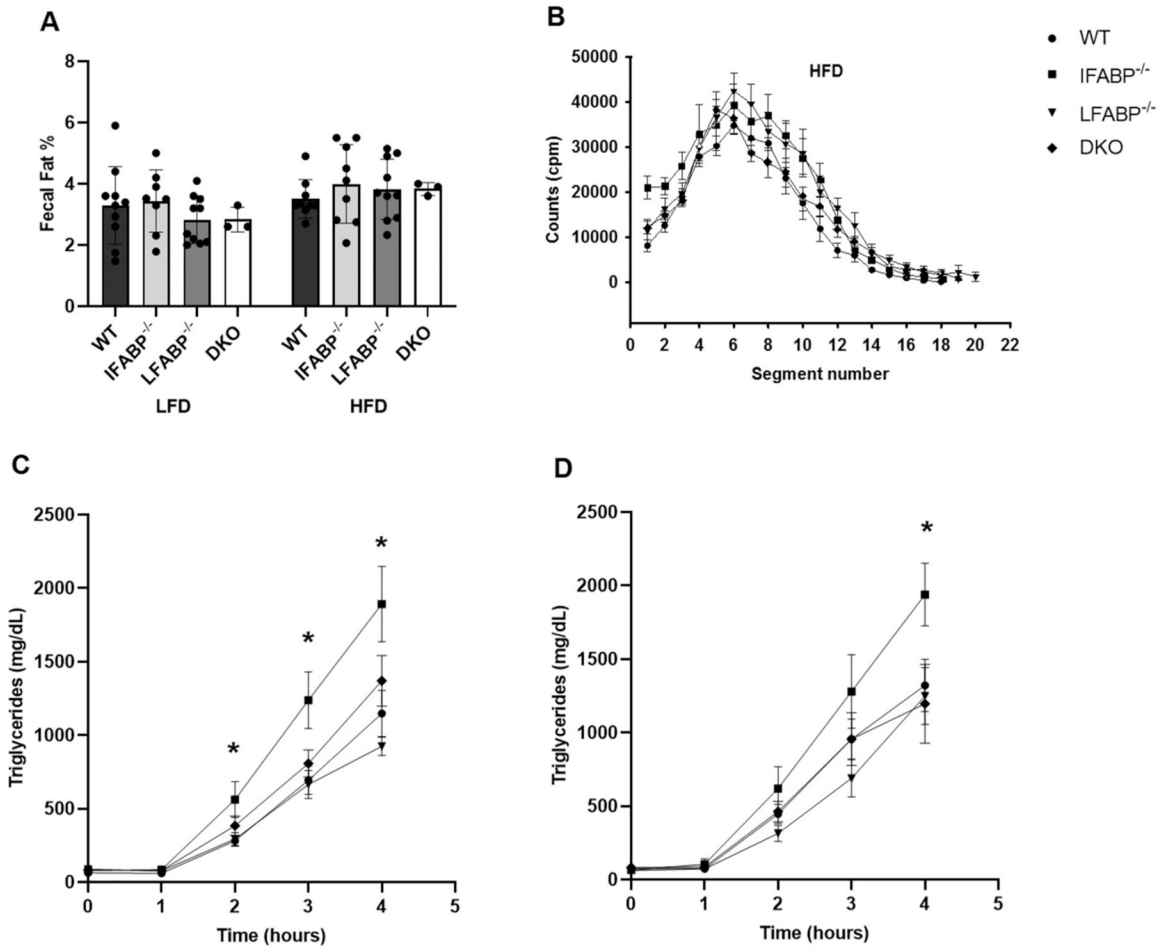

Fig. 7.

Intestinal lipid uptake and secretion for WT (●), IFABP$^{-/-}$ (■), LFABP$^{-/-}$ (▾), and DKO (◆) mice after 12 weeks on a low-fat (LFD) or high saturated fat (HFD) diet. A. Fecal lipid % for LFD or HFD-fed mice (n = 3–10); B. Intestinal lipid uptake of HFD-fed mice; C. Oral fat tolerance test for LFD-fed mice (n = 6–11); D. Oral fat tolerance test for HFD-fed mice (n = 8–12); Data are given as mean ± SD in A; mean ± SEM in B, C and D, analyzed using Student's t-test *$p < 0.05$ for IFABP$^{-/-}$ vs WT at the same timepoint.

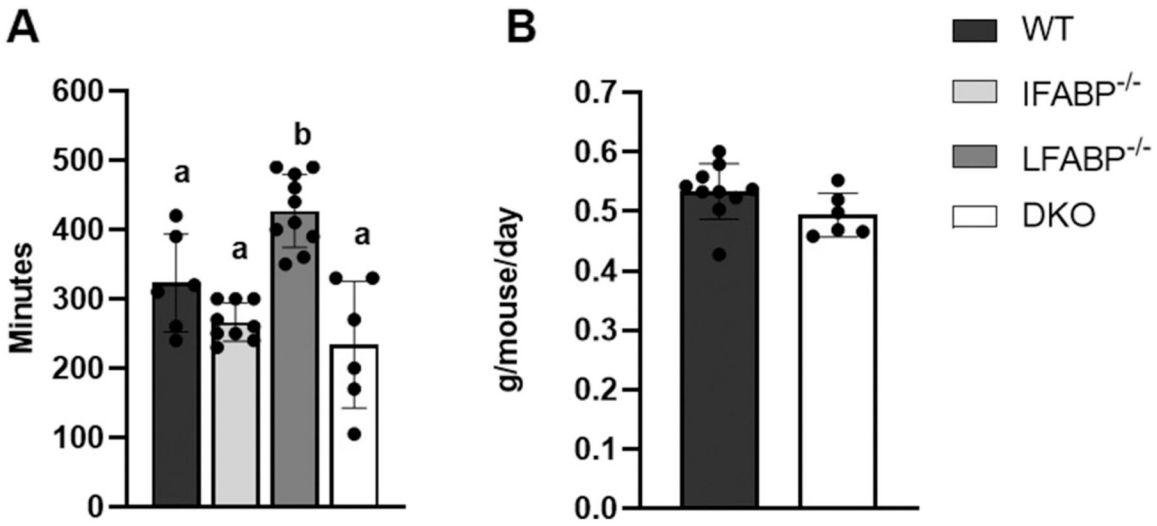

Fig. 8.

The intestinal transit time in WT, IFABP$^{-/-}$, LFABP$^{-/-}$, and DKO mice after 12 weeks on a high saturated fat diet. A. Intestinal transit time (n = 6–10); B. Fecal output (n = 6–10). For fig. A, data are mean ± SD, analyzed using one-way ANOVA with Tukey's post hoc test. Results with different letters are significantly different ($p < 0.05$). For fig. B, data are given as mean ± SD, analyzed using Student's *t*-test. n = 6–10.

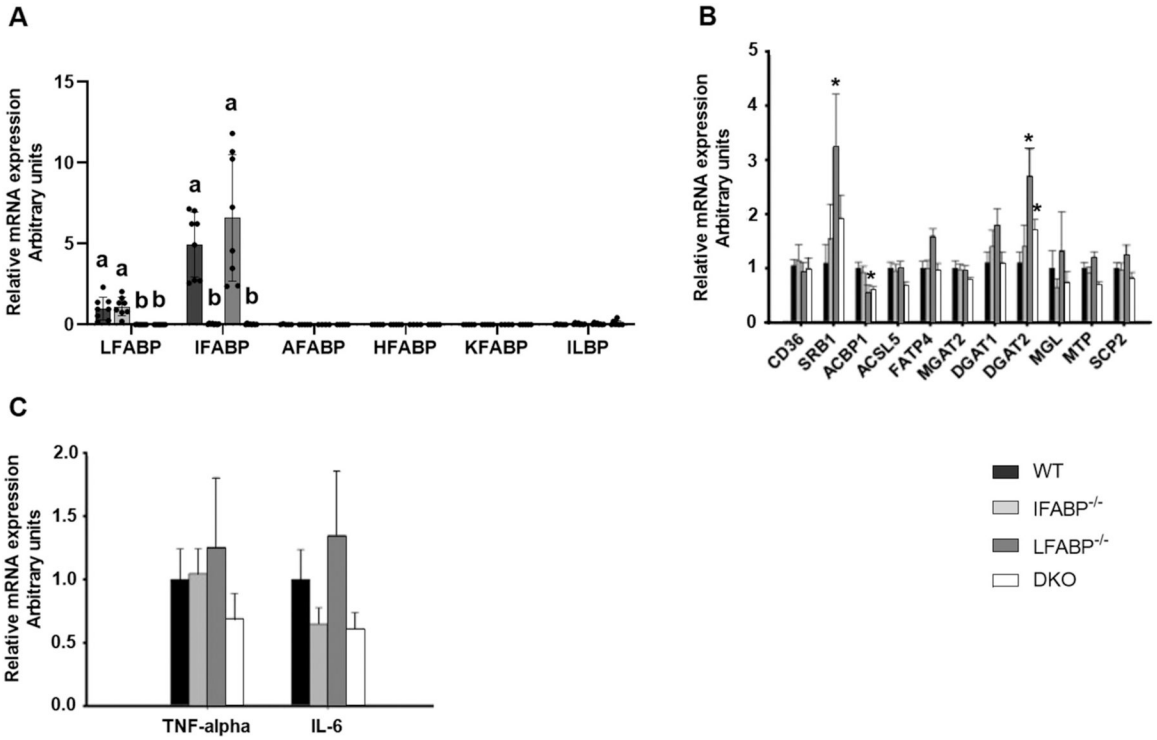

Fig. 9.

Relative quantification of mRNA expression of intestinal lipid transport genes for WT, IFABP$^{-/-}$, LFABP$^{-/-}$ and DKO mice after 12 weeks on a high saturated fat (HFD) diet. A. mRNA expression of different FABPs relative to intestinal LFABP in WT mice (n = 4–8); B. Relative expression of intestinal lipid transport genes; C. Relative expression of inflammatory cytokines in the intestine. Data are given as mean ± SD in A and mean ± SEM in B and C, and are analyzed using Student's t-test. Results with different letters vs the same WT are significantly different ($p < 0.05$). *p < 0.05 vs WT.

Biochim Biophys Acta Mol Cell Biol Lipids. Author manuscript; available in PMC 2023 July 01.

Table 1

Plasma and tissue analyses for WT, IFABP$^{-/-}$, LFABP$^{-/-}$ and DKO mice after 12 weeks on LFD, or HFD diet.

	LFD				HFD			
	WT	**IFABP$^{-/-}$**	**LFABP$^{-/-}$**	**DKO**	**WT**	**IFABP$^{-/-}$**	**LFABP$^{-/-}$**	**DKO**
Glucose, mg/dL	131 ± 9	90 ± 6	137 ± 17	122 ± 14	184 ± 15^{b}	104 ± 4^{a}	218 ± 16^{b}	178 ± 16^{b}
Insulin, ng/mL	0.33 ± 0.10	0.35 ± 0.02	0.26 ± 0.02	0.36 ± 0.02	0.24 ± 0.02	0.17 ± 0.01	0.17 ± 0.01	0.24 ± 0.02
HOMA, IR	3.1 ± 0.6	2.0 ± 0.2	2.3 ± 0.4	2.7 ± 0.3	2.5 ± 0.1^{b}	1.1 ± 0.1^{a}	2.4 ± 0.3^{b}	2.7 ± 0.4^{b}
Total cholesterol, mg/dL	77 ± 6	67 ± 3	65 ± 8	62 ± 5	102 ± 11	100 ± 5	112 ± 6	106 ± 3
TG, mg/dL	35 ± 5	22 ± 5	43 ± 4	33 ± 5	27 ± 4	55 ± 14	38 ± 14	47 ± 5
NEFA, mEq/L	0.23 ± 0.03^{a}	0.26 ± 0.01^{ab}	0.36 ± 0.03^{b}	0.28 ± 0.03^{ab}	0.25 ± 0.03^{a}	0.35 ± 0.02^{ab}	0.44 ± 0.05^{b}	0.40 ± 0.03^{b}
BHB, mg/dL	–	–	–	–	13.3 ± 0.9^{b}	11.4 ± 1.7^{ab}	12.0 ± 0.8^{ab}	9.2 ± 0.8^{a}
Leptin, ng/mL	1.5 ± 0.8	0.3 ± 0.1	2.6 ± 0.8	2.2 ± 0.6	3.7 ± 0.8^{b}	0.8 ± 0.3^{a}	8.6 ± 1.5^{c}	6.8 ± 1.3^{bc}
Leptin Index	0.3 ± 0.1	0.1 ± 0.0	0.4 ± 0.1	0.5 ± 0.2	0.6 ± 0.1^{b}	0.2 ± 0.1^{a}	0.9 ± 0.1^{b}	0.9 ± 0.1^{b}
Adiponectin, ng/mL	10.0 ± 0.7	7.6 ± 0.6	10.9 ± 1.1	9.6 ± 1.2	8.8 ± 0.0^{b}	4.6 ± 0.2^{a}	7.1 ± 0.6^{b}	6.9 ± 0.5^{ab}
Adiponectin Index	3.3 ± 0.5	2.8 ± 0.3	2.0 ± 0.4	2.3 ± 0.5	1.8 ± 0.3^{b}	1.6 ± 0.2^{ab}	0.8 ± 0.1^{a}	0.9 ± 0.1^{a}
Intestine length, cm	34 ± 1^{ab}	32 ± 0^{a}	34 ± 0^{ab}	35 ± 1^{b}	36 ± 1^{ab}	35 ± 0^{a}	37 ± 0^{bc}	39 ± 0^{c}
Liver Wt, g	0.85 ± 0.03	0.84 ± 0.02	0.93 ± 0.03	0.84 ± 0.02	0.93 ± 0.04	0.92 ± 0.03	0.96 ± 0.04	0.90 ± 0.03
Liver, g/g BW	0.034 ± 0.004^{b}	0.034 ± 0.001^{b}	0.034 ± 0.001^{ab}	0.031 ± 0.001^{a}	0.035 ± 0.001^{b}	0.035 ± 0.001^{b}	0.030 ± 0.001^{a}	0.030 ± 0.000^{a}
Epididymal fat, g	0.37 ± 0.05^{a}	0.26 ± 0.05^{a}	0.68 ± 0.07^{b}	0.61 ± 0.05^{b}	0.78 ± 0.11^{b}	0.29 ± 0.03^{a}	0.98 ± 0.11^{b}	0.85 ± 0.06^{b}
Perirenal fat, g	0.09 ± 0.02^{a}	0.08 ± 0.02^{a}	0.19 ± 0.02^{b}	0.18 ± 0.02^{b}	0.23 ± 0.04^{b}	0.08 ± 0.01^{a}	0.39 ± 0.04^{c}	0.28 ± 0.03^{bc}
Inguinal fat, g	0.35 ± 0.08^{ab}	0.22 ± 0.03^{a}	0.56 ± 0.05^{c}	0.42 ± 0.04^{bc}	0.43 ± 0.06^{b}	0.20 ± 0.03^{a}	0.73 ± 0.07^{c}	0.71 ± 0.06^{c}

Data are mean ± S.E.M and analyzed using one-way ANOVA with Tukey's post hoc test. Results with different letters within a dietary treatment are significantly different ($p < 0.05$). $n = 6–9$ for all groups.